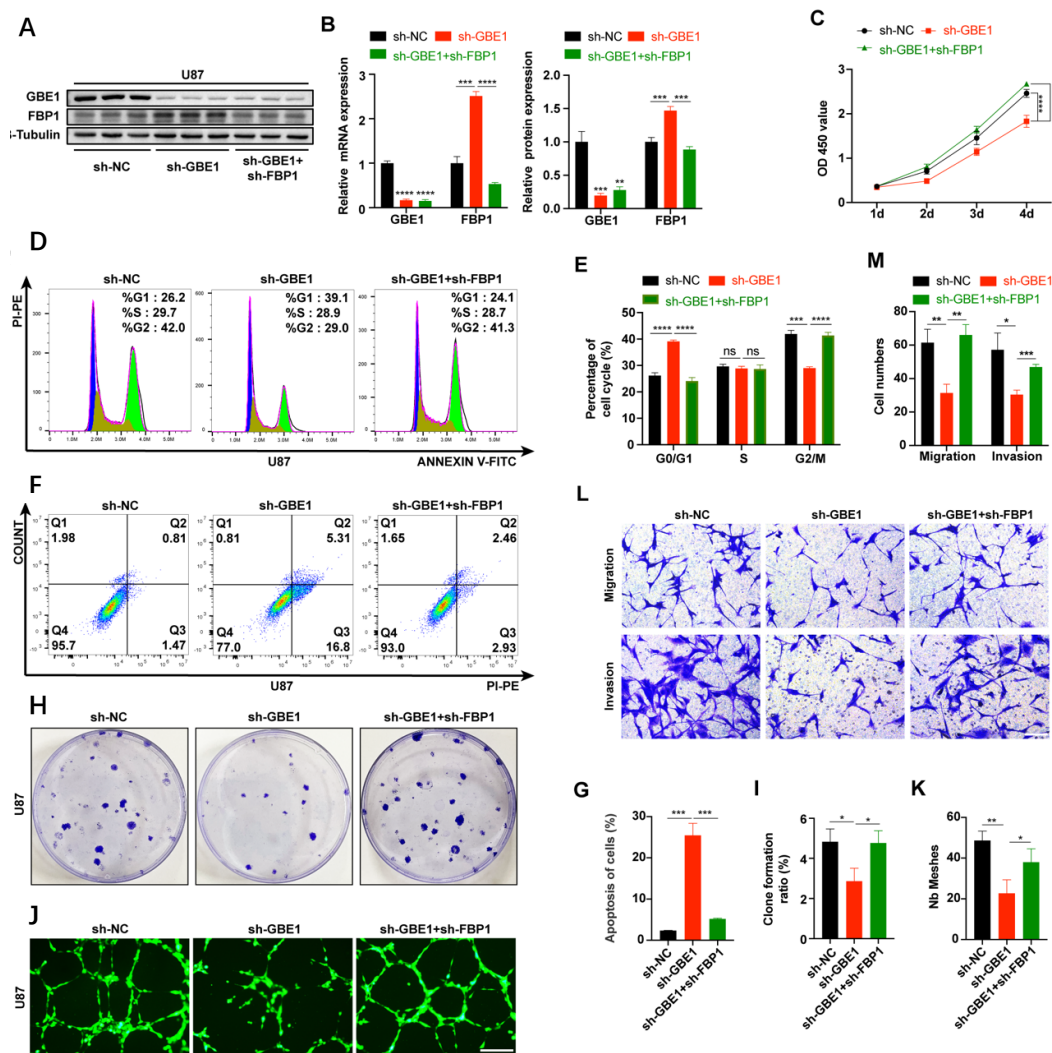


## Supplementary Figures



**Figure S1.** FBP1 knockdown in U87 cells reversed the tumor suppression caused by GBE1 knockdown. (**A**, **B**) Knockdown efficiency of sh-GBE1 and sh-GBE1 + sh-FBP1 in U87 cells (n = 3). (**C**) The viability of U87 cells infected with sh-GBE1 or sh-GBE1 + sh-FBP1 (n = 6). (**D**, **E**) Cell cycle analysis and (**F**, **G**) apoptosis analysis of U87 cells infected with sh-GBE1 or sh-GBE1 + sh-FBP1 (n = 3). (**H**, **I**) Colony formation ability, (**J**, **K**) angiogenic ability, (**L**, **M**) migration and invasion ability of U87 cells with both GBE1 and FBP1 knockdown; colony forming ability was evaluated by colony formation assay (n = 3); colony formation ratio = amount of colonies/number of seeded cells; angiogenic capacity was assessed by tube formation assay and representative images at 12 h were selected for presentation (n = 3); scale bar: 250  $\mu$ m; migration and invasion abilities were evaluated by Transwell assay (n = 3); five fields from top to bottom were selected for each chamber, and the average number of cells from three independent experiments was calculated. Scale bar: 100  $\mu$ m. Data are presented as mean  $\pm$  SD (ns P > 0.05; \*P < 0.05; \*\*P < 0.01; \*\*\*P < 0.001; \*\*\*\*P < 0.0001).